Title	Monitoring local unfolding of bovine serum albumin during denaturation using steady-state and time-resolved fluorescence spectroscopy
Author(s)	Togashi, Denisio M.; Ryder, Alan G.; O'Shaughnessy, Domhnall
Publication Date	2010-03
Publication Information	Togashi, D.M.; Ryder, A.G.;O'Shaughnessy, D.; (2010) 'Monitoring Local Unfolding of Bovine Serum Albumin During Denaturation Using Steady-State and Time-Resolved Fluorescence Spectroscopy'. Journal Of Fluorescence, 20 :441-452.
Publisher	Springer
Link to publisher's version	http://dx.doi.org/10.1007/s10895-009-0566-8
Item record	http://hdl.handle.net/10379/5503
DOI	http://dx.doi.org/DOI 10.1007/s10895-009-0566-8

Published as: Monitoring Local unfolding of Bovine Serum Albumin during denaturation using steady-state and time-resolved fluorescence spectroscopy. D.M. Togashi, A.G. Ryder, and D. O'Shaughnessy, *Journal of Fluorescence*, 20(2), 441-452, **(2010)**.
DOI: 10.1007/s10895-009-0566-8

Monitoring local unfolding of Bovine Serum Albumin during denaturation using steady-state and time-resolved fluorescence spectroscopy.

Denisio M. Togashi*, Alan G. Ryder, and Domhnall O'Shaughnessy

Nanoscale Biophotonics Laboratory. School of Chemistry,

National University of Ireland, Galway. Galway, Ireland.

*Correspondence to: Dr. Denisio M. Togashi, Nanoscale Biophotonics Laboratory, School of Chemistry, National University of Ireland-Galway. Co. Galway. Ireland. Tel. +351(0) 91493144, Fax +351(0) 91 52 5700.
Email: denisio.togashi@nuigalway.ie

Abstract

In a previous report (*J. Fluoresc*. 16, 153, 2006) we studied the chaotropiclly induced denaturation of Bovine Serum Albumin (BSA) using the fluorescence decay kinetics at different stages in the denaturation of BSA by guanidinium hydrochloride (GuHCl). In this work, we gain a more detailed insight into the BSA denaturation process by investigating the thermodynamics of the process. Structural changes were monitored spectrophotometrically via the intrinsic protein fluorescence from tryptophan residues, and the extrinsic fluorescence from 1,8-anilinonaphthalene sulphonate (ANS). ANS tends to locate in a variety of binding sites in BSA which are located in different domains, and these can be selectively populated using different, 1:1 and 1:10 molar ratios of BSA to ANS. The data from steady-state and time-resolved fluorescence spectroscopy were analyzed using thermodynamic two-state and three-state models and the lifetime data clearly indicated the formation of an intermediate state during denaturation. A global analysis using non-linear regression gave a $\Delta G^0_{H_2O,D}$ = 6.7 kcal.mol^{-1} for the complete unfolding of the BSA-ANS complexes, and a $\Delta G^0_{H_2O,I}$ = 0.9 kcal.mol^{-1} for the first step to the intermediate. Therefore, the unfolding energy of the intermediate, which appears mostly at intermediate GuHCl concentrations (1.0 to 1.5 M), to the denatured state, is 5.8 kcal.mol^{-1}. The lifetime analysis of the BSA-ANS complexes also shows clearly that there are differences in stability of the BSA domains, with domain III unfolding first at low GuHCl concentrations (<1.5M).

Keywords: Protein, Bovine Serum Albumin, Fluorescence, ANS, Gaussian lifetime distribution, Three-state transition model.

Introduction

Proteins are important for the structure, function, and regulation of cells, tissues, and organs and every protein has a unique function in maintaining life. Proteins are biopolymer molecules that may be distinguished from each other by the difference in amino acid unit sequence which composes the protein primary structure. The transformation of this polypeptide chain into a

specific and distinctive three-dimensional, folded native state, gives rise to biological function of great selectivity and variety. One of major endeavours in molecular biology is the investigation of the mechanism of protein folding/unfolding/refolding [1]. Small changes in the local environment of a protein can cause structural changes leading to the formation of alternate conformations and thereby, affect the original function of the protein. More significantly, defects in native state protein folding may be the molecular basis for a wide range of human genetic disorders. In the case of rare neurodegenerative illnesses in mammals such as Alzheimer's and Parkinson's diseases [2,3], misfolded, and/or partially unfolded protein states compete with the normally folded protein leading to adverse effects. As a result, considerable attention has been devoted to characterizing partially unfolded protein states in order to gain more information on the sequence and steps involved in protein folding mechanisms. The non-contact, non-destructive observation and monitoring protein folding is also of interest where protein adsorption occurs on surfaces, and in particular for understanding how different biomaterials interact with plasma proteins.

Denaturation does not affect the primary structure of protein but it disrupts both the secondary and tertiary structures of proteins, *i.e.*, total or partial loss of three-dimensional structure. Proteins can be denatured by heat, pH, or chemical denaturants such as Guanidinium hydrochloride (GuHCl), a chaotropic denaturant [4]. Denaturing agents, when used under relatively mild conditions, weaken or break only the non-covalent interactions such as, hydrogen bonds or salt bridges, which are responsible for the tertiary protein structure. Partially folded intermediates have been observed during the folding process for a number of proteins under *in-vitro* conditions [5]. The intermediate states of unfolding/refolding mechanisms may thus be studied via the denaturation of proteins. The complexity of the denaturation process becomes more evident when the protein contains multidomain structures in which each domain can unfold (in)dependently and, the association of different domains in the whole protein through various short-range and long-range interactions may affect the overall process [6,7].

The denaturation process can be followed using a variety of different experimental approaches [4,5]. Fluorescence spectroscopy is a reliable tool in the study of proteins due to its great sensitivity and selectivity. In many cases, the protein of interest will contain one or more amino acids that are intrinsically fluorescent (phenylalanine, tyrosine, or tryptophan). The emissions of these intrinsic fluorophores are environmentally sensitive (generally via polarity) and this conveniently allows the denaturation process to be followed. The use of extrinsic fluorophores attached to the protein can further extend the possible range of protein denaturation studies in particular where an intrinsic fluorescent amino acid is not present [8,9]. Geometrical effects can be successfully quantified using fluorescence resonance energy transfer (FRET) where the changes in distance between donor and acceptor centres can be monitored [10]. Therefore, by using fluorescence probes which can be selectively attached to various protein domains and analysing the changes in spatial distance between these probes using FRET, a clearer picture of the protein structural alterations in course of a denaturation process can be obtained [11-13]. 1-anilino-8-naphthalene sulphonate (ANS) is a well known protein probe [14-,16], and we have made extensive use of this extrinsic probe in our studies of BSA properties [10,17] and denaturation [9].

Serum albumin is the most abundant of all the proteins in blood plasma, accounting for approximately 60% of the total serum protein content. The secondary structure of the polypeptide chain consists of about 580 amino acids with approximately 67% present as alpha-

DOI: 10.1007/s10895-009-0566-8

helices without beta-sheets (see structure model in Fig. 1). The protein is composed of three homologous domains (I, II, and III) which are divided into two sub-domains (A and B). In addition, there are nine loops and 17 disulphide bridges, which make a heart-shaped 3D structure of the protein molecule [18,19]. The principal function of serum albumin is to transport a great variety of fatty acids and metabolites [19] via the main binding regions located in sub-domains IIA (Site 1) and IIIA (Site 2) [19,20]. Human and Bovine Serum Albumins (HSA and BSA, respectively) are probably the most studied serum albumin proteins. They exhibit approximately 76% homology and a repeating pattern of disulphides which are strictly conserved [18,19]. The main difference between the two proteins is that in HSA there is only one tryptophan amino acid which is located at position 214 (equivalent to Trp-212 for BSA), buried in a hydrophobic pocket at sub-domain IIA; whereas in BSA an additional tryptophan amino acid Trp-134, which is more exposed to solvent, is found at sub-domain IB [18,19]. When GuHCl is used to induce protein unfolding in serum albumins it has led to the reporting of contradictory results in the literature with regard to the exact unfolding mechanism. There are reports that point induced unfolding HSA occurs in a single step [13,21-24] while other studies indicate a multi-step process with the formation of stable intermediates [25-29].

In this work, we gain more insight into the denaturation process of the protein Bovine Serum Albumin (BSA) induced by GuHCl. The structural changes are monitored spectrophotometrically *via* protein fluorescence emission from the intrinsically fluorescent tryptophan residues, and extrinsic fluorescent probe ANS associated to BSA at two different molar ratios (1:1 and 1:10). A detailed analysis of the GuHCl induced denaturation is provided as well as determination of the thermodynamics involved in the process.

Experimental.

Materials:

Bovine serum albumin (BSA) of purity 99+ % (catalogue no. A7638) and GuHCl were purchased from Sigma, and 8-Anilino-1-naphthalenesulphonic acid hemi-magnesium salt hydrate (ANS) of purity 90+% purchased from Fluka. All reagents were used without further purification. Phosphate buffered saline tablets for 0.01 M phosphate buffer (PBS), 0.0027 M potassium chloride and 0.137 M sodium chloride at pH 7.4 was purchased from Aldrich. All solutions were made up in purified water from a Milli-Q Millipore system.

Sample preparation:

Fresh protein solutions were made up daily in PBS at pH=7.4 were used for experimental work. A stock ~ 1 mM ANS aqueous solution and 8 M GuHCl in PBS were also prepared. The appropriate amounts of protein and ANS were mixed and incubated in the dark at room temperature for 2 hr. The BSA and ANS concentration was calculated using molar extinction coefficients ε_{280} = 43600 M^{-1} cm^{-1} [14] and ε_{350}= 5000 M^{-1} cm^{-1} [14], respectively. The BSA-ANS solutions were then mixed with a series of GuHCl concentration in PBS. These solutions were then incubated overnight (~ 8 hours) in the dark at room temperature prior to measurement. The final protein concentrations were less than ~ 2 x 10^{-6} M for all fluorescence measurements, in order to keep the optical density below 0.06.

Instrumentation:

Absorption spectra were recorded using a Shimadzu UV-1601 UV-visible spectrophotometer and steady state fluorescence emission and excitation measurements on LB50 Perkin Elmer and

DOI: 10.1007/s10895-009-0566-8

Cary Eclipse spectrofluorimeters, in 2 and 10 mm pathlength cells at room temperature. Magic-angle fluorescence decays were recorded using a Time Correlated Single Photon Counting (TCSPC) Fluotime 200 system using a pulsed laser diode (405 nm) excitation source (Picoquant GmbH). The repetition rate of the excitation laser was fixed at 5 MHz and decays obtained at a time resolution of 70 ps. Typical full widths at half-maximum obtained for instrument response function were in the order of a hundred picoseconds.

Data analysis:

Denaturation models

The two-state model (N⇌D) is a simple but very useful model used to interpret and extract thermodynamic parameters for protein denaturation [4, 30]. The dependence of the free energy change of the denaturation (ΔG_D^0) with the guanidinium hydrochloride (GuHCl) concentration is described as:

$$\Delta G_D^0 = -RT \ln \frac{[D]}{[N]} = \Delta G_{H_2O,D}^0 + m_D \cdot [GuHCl] \quad (1)$$

Where $\Delta G_{H_2O,D}^0$ is the free energy of denaturation without the denaturant and, m_D accounts for the degree of strength of the denaturant. R is the gas constant, T is the temperature (298K), $[D]$ is the concentration of unfolded protein and $[N]$ is the concentration of folded protein. By using the unfolded molar fraction, $x_D=[D]/([D]+[N])$, equation (1) is rearranged to:

$$x_D = \frac{e^{-\Delta G_D^0/RT}}{1+e^{-\Delta G_D^0/RT}} \quad (2)$$

with the native molar fraction (x_N) equal to $1-x_D$. The fluorescence intensity at 350 nm (Trp emission) and at 480 nm (ANS emission) was measured using excitation wavelength at 295 nm and at 380 nm, respectively. All fluorescence spectra were corrected for background fluorescence by subtracting a blank PBS buffer solution spectrum. The fluorescence intensity of protein in the presence of denaturant (I_{GuHCl}) can be calculated from the fluorescence intensities of the protein without denaturant (I_N), and the fully unfolded protein (I_D), via:

$$I_{GuHCl} = x_N \times I_N + x_D \times I_D \quad (3)$$

In the Santoro and Bolen approach [4,30] for denaturation studies, the equations 4 and 5 are used:

$$I_N = I_N^0 + \alpha_N [GuHCl] \quad (4)$$

$$I_D = I_D^0 + \alpha_D [GuHCl] \quad (5)$$

The parameters I_N^0, I_D^0, α_N, and α_D account for baseline effects at the start and end of the denaturation isotherm. I_N^0 and I_D^0, represent the intercepts of the intensity extrapolated to zero denaturant concentration for the native and unfolded states, while α_N, and α_D the slopes for the

DOI: 10.1007/s10895-009-0566-8

dependencies of I_N and I_D on denaturant concentration. Therefore, I_{GuHCl} is obtained by the introduction of eq. 1-2, and eq. 4-5 into equation 3:

$$I_{GuHCl} = \frac{I_N^0 + \alpha_N[GuHCl] + \left(I_D^0 + \alpha_D[GuHCl]\right)\exp[-\left(\Delta G_{H_2O}^0 + m_D[GuHCl]\right)/RT]}{1 + \exp[-\left(\Delta G_{H_2O}^0 + m_D[GuHCl]\right)/RT]} \quad (6)$$

For the three-state model, additional parameters for the presence of an intermediate, *I*, are needed to describe the total fluorescence intensity of the protein at different stages of the unfolding process. This can be described as:

$$I_{GuHCl} = x_N \times I_N + x_I \times I_I + x_D \times I_D \quad (7)$$

Where, x_I and I_I are the molar fraction and the fluorescence intensity of the intermediate in the equilibrium N⇌I⇌D [4, 31]. It is also assumed that there is a linear relationship between I_I and the guanidinium hydrochloride concentration ($I_I = I_I^0 + \alpha_I[GuHCl]$), and that the total fluorescence intensity of the protein, in the three-state model for each denaturant concentration (I_{GuHCl}) can be calculated by incorporating equation 7 into equation 8:

$$I_{GuHCl} = \frac{\begin{array}{c} I_N^0 + \alpha_N[GuHCl] + \left(I_I^0 + \alpha_I[GuHCl]\right)\exp[-(\Delta G_{H_2O,I}^0 + m_I[GuHCl])/RT] + \\ \left(I_D^0 + \alpha_D[GuHCl]\right)\exp[-(\Delta G_{H_2O,D}^0 + m_D[GuHCl])/RT] \end{array}}{1 + \exp[-(\Delta G_{H_2O,I}^0 + m_I[GuHCl])/RT] + \exp[-(\Delta G_{H_2O,D}^0 + m_D[GuHCl])/RT]} \quad (8)$$

where, $\Delta G_{H_2O,I}^0$ and $\Delta G_{H_2O,D}^0$ are the free energies of denaturation in the absence of denaturant for the native structure to intermediate (I), and for the native structure to the fully denatured state (D), respectively. The parameters that account for the degree of strength of the denaturant for N⇌I and N⇌D, in the three-state model, are m_I and m_D, respectively.

Fluorescence Intensity decays:

For the analysis of the fluorescence decay data from we have used a combination of a single Gaussian distribution and a single discrete decay times:

$$I(t) = a_1 \int_0^\infty \rho(\tau) e^{-t/\tau} d\tau + a_2 \exp(-t/\tau_2) \quad (9)$$

where

$$\rho(\tau) = \frac{1}{\sigma_1\sqrt{2\pi}} \exp\left[-\frac{1}{2}\left(\frac{\tau - \tau_1}{\sigma_1}\right)^2\right] \quad (10)$$

The parameters a_1 and a_2 are the amplitude of each term in equation 9, τ_1 is the mean decay time of the Gaussian distribution with a standard deviation of σ_1. The full width at half maximum (FWHM) of a Gaussian distribution is given by $2.345\sigma_1$, and we will hereafter refer to σ_1 as the width of the distribution. τ_2 is the lifetime of the discrete, single exponential term in equation 9. The model was implemented in the analysis program via a nonlinear least-squares procedure based on the Marquardt-Levenberg algorithm and combined with an iterative reconvolution

DOI: 10.1007/s10895-009-0566-8

method based on the fast Fourier transform (FFT) to account for distortions of the decay signal from the instrument response function. The quality of the fittings was judged using the usual statistical criteria: symmetrical distribution of weighed residuals for the autocorrelation function and the chi squared (χ^2) parameter.

Results and Discussion

Steady state analysis of BSA and BSA-ANS denaturation

Denaturation of BSA using GuHCl (figure 2) and BSA-ANS complexes (figure 3) was monitored by changes in fluorescence spectra. The effect of GuHCl addition on the tryptophan (Trp) fluorescence emission in BSA shows various changes in intensity and wavelength of the fluorescence band maxima. The Trp fluorescence intensity is found to first increase with GuHCl concentrations below 0.5 M, and then decrease dramatically at higher concentrations in particular between 2.0 M and 5.0 M. The wavelength shift is also bimodal, with a slight blue shift (< 1.5 nm) of the 349 nm Trp band with increasing GuHCl concentrations up to 2.0 M, followed by a red shift to ~ 356 nm at higher concentrations.

The blue shift at relatively low GuHCl concentrations has been observed previously for BSA (between 0.1-1.6 M) [32] and HSA (below 1.2 M) [25]. The close similarity in behaviour of both proteins at this GuHCl concentration range (below 2.0 M), indicates that, it is the Trp-214 and Trp-212 located in domain II, respectively, for HSA and BSA (see Fig. 1) that are most affected by the presence of the denaturant. This small blue shift and fluorescence intensity increase can be caused by the movement of Trp-212 to the less polar, inner core of the hydrophobic cavity in sub-domain IIA which is the Binding Site 1 location. This movement may be triggered by either a partial rearrangement of domain II, or a change in the separation of domains II and III which in turn alters the packing structure of domain II. With further addition of denaturant (> 2 M), the big fluorescence intensity drop and red shift of the Trp fluorescence emission is clear evidence that the Trp-212 is more exposed to a more polar environment allowing water molecules to quench the fluorescence, or quenching by other aminoacid residues which can become close to the tryptophan [32-35]. This is clear evidence that domain II is now being unfolded to a very significant degree. Using the Trp fluorescence intensity data, a denaturation isotherm can be plotted (fig. 4a) which indicates that a single transition process (two-state model) is operating. However, from the spectral shift and the intensity change data of the Trp emission, one would expect that the unfolding process is a two-step mechanism.

Analysis of the unfolding equilibria of unlabeled BSA using Trp emission data was done using the Santoro and Bolen approach for a two-state transition model, equation 6 [4,30] and three-state transition model (equation 8). The 3 state model would not converge to physically-meaningful values, and so was discarded, while the 2 state model fitted the data well (Fig. 4a) and thermodynamic parameters (Table 1) were obtained. The $\Delta G^0_{H_2O,D}$ and $-m_D$ of BSA unfolding were found to be 4.5 kcal/mol and 2.5 kcal/mol.M, respectively. These values are in agreement with 3.4 kcal/mol to 4.85 kcal/mol for $\Delta G^0_{H_2O,D}$, and 0.45 kcal/mol.M to 3.6 kcal/mol.M for $-m_D$ found for HSA denaturation using a two-state transition mechanism [13,21-24]. It is possible that the fluorescence intensity changes observed for the tryptophan at GuHCl concentration of < 2.0 M are too small to overcome the differences between the two and three-state model.

DOI: 10.1007/s10895-009-0566-8

The BSA denaturation was also studied using an extrinsic ANS fluorophore label at two different molar ratios of 1:1 and 1:10. The normalised fluorescence emission of tryptophan, 315-415 nm (Fig. 3a) and ANS, 400-700 nm (Fig. 3b) for the 1:10 BSA-ANS complex both show a clear red-shift with increasing GuHCl concentration similar to the unlabelled BSA case [36]. The effect of denaturant on the fluorescence spectra observed for the 1:1 and 1:10 BSA-ANS molar ratios were similar. ANS molecules can bind to the BSA protein in up to five different binding sites of various affinities and polarities [9,10], with the ANS fluorescence increasing substantially when the fluorophores are bound in the more hydrophobic sites on the protein [14-16].

For Trp emission from the BSA-ANS complexes, a similar pattern is observed during denaturation as was seen for the unlabelled BSA, i.e. first a blue shift with low GuHCl concentrations followed by a red shift in Trp emission. When the BSA-ANS complex is excited at 380 nm, a red shift to ~ 475 nm, a decrease in intensity, and a broadening of the ANS emission band is observed with increasing GuHCl concentration (Fig. 3b). This can be explained by the opening up of the hydrophobic pockets during the denaturation process [9], and so the ANS binding sites become more water exposed and the ANS fluorescence band becomes similar to the free ANS fluorescence band in aqueous solution as shown by the dashed line almost overlapping with the grey line (highest GuHCl concentration) in figure 3b. One however, cannot ignore the possibility, that there is also a concommitant weakening of the ANS binding interaction leading to a release of free ANS. This could occur via decreases in either the association constant or number of ANS proteins binding caused by the increasing GuHCl concentration.

Plotting the denaturation isotherms for the BSA-ANS complexes using Trp emission when excited at 295 nm (Fig 4a) or ANS emission when excited using 380 nm (Fig 4b) shows some significant differences. In Fig 4a where changes in Trp emission intensity are plotted, the BSA-ANS complexes are very different with respect to the unlabelled case. In the 1:1 BSA-ANS complex, the initial Trp intensity (in absence of GuHCl) is decreased by more than 20%, while the 1:10 BSA-ANS complex shows a reduction of more than 90%. This is due to intermolecular Förster Resonance Energy Transfer (FRET) from Trp to ANS, and the effect is obviously much stronger when there are more ANS acceptors as with the 1:10 complex [10]. The Trp emission band overlaps strongly with the absorption band of ANS, giving an efficient FRET effect and a Förster radius of about 24 Å [10].

When GuHCl concentration increases up to 0.5-1.0 M, we see a gradual increase in the Trp fluorescence intensity for the 1:1 BSA-ANS complex. Further GuHCl concentration increases (1.5 M to 2.0 M in particular) causes the fluorescence intensity of the 1:1 BSA-ANS complex to significantly decrease, while above 2.5 M the intensity is constant for the unlabelled, 1:1, and the 1:10 BSA-ANS complexes. In the 1:10 complex, the Trp fluorescence intensity increases 3-fold as the denaturant concentration approaches ~ 1.5 M, however, the maximum intensity attained is still far less than either the unlabelled BSA or 1:1 BSA-ANS complex.

The increase of tryptophan emission may be explained by either an increase in the distance between the tryptophan residues and the ANS binding sites or a decrease in ANS bound near to these residues. In contrast to the unlabeled BSA case, Trp fluorescence intensity changes in the BSA-ANS complexes in the low GuHCl concentration range (<1.5 M) are much more significant in magnitude because of the observed FRET. This information can thus be used to better define the local protein structure unfolding where these tryptophan and ANS binding sites are located. For GuHCl concentrations above 1.5 M, the decrease in Trp fluorescence intensity in both

DOI: 10.1007/s10895-009-0566-8

complexes seems to be due to the single transition-state unfolding process as observed for the unlabeled protein (*vide infra*).

The normalised denaturation isotherms for 1:1 and 1:10 BSA-ANS complexes generated from the ANS emission (Fig. 4b) show a near linear decrease in the fluorescence intensities, with increasing GuHCl concentration, up to ~ 0.8 M, a shallow saddle between 0.8 M and ~ 1.5 M, and then a steep decline between ~ 1.5 to ~ 2.2 M GuHCl concentration, after which the intensity levels off almost to zero. There is a significant difference in the normalised denaturation isotherms according to the amount of ANS bound to BSA, with 1:10 complex having intermediates points with greater fluorescence emission and a more pronounced saddle at intermediate GuHCl concentrations. These differences may be due to the difference in the ANS binding sites in the different domains presented in BSA [10].

Fluorescence data from Trp and ANS when analysed indicate that denaturation of the ANS-BSA complex is occurring via two apparently different processes, which is implausible. It therefore seems reasonable to globally analyse the denaturation isotherms by applying a three-state model (we show later that this is a valid assumption). Therefore, using equation 8, the thermodynamic parameters that best fit globally all the experimental data for a total of ten denaturation isotherms are obtained (Table 1). The baseline slope parameters (α_I and α_D) were assumed to be zero while the other parameters in the model fitting were allowed to freely change independently of each other to achieve the best fit. The results show a good match between the experimental data and the model fitting curves (figure 4). Non-linear regression global analysis of the data yielded that the energy for the first step and the total process of BSA-ANS unfolding is $\Delta G^0_{H_2O,I}$ = 0.9 kcal.mol^{-1} and $\Delta G^0_{H_2O,D}$ = 6.7 kcal.mol^{-1}, respectively. Therefore, the unfolding energy of the intermediate, which appears mostly at intermediate GuHCl concentrations (1.0-1.5 M), is 5.8 kcal.mol^{-1}. It is interesting to note that using Trp fluorescence data from the unlabeled BSA with a two-state model yields an unfolding energy of 4.5 kcal.mol^{-1}.

Fluorescence studies of the HSA-ANS complex have shown that ANS is primarily bound to hydrophobic sites in sub-domain IIIA with a smaller proportion located in lower affinity sites of sub-domain IIA [37]. A more detailed FRET study of BSA-ANS complexes, showed that there were up to five different binding sites for ANS in BSA and provided a quantitative relationship between the different binding sites (and constants) to the distance between the binding site and the tryptophan residues [10]. The highest affinity binding site (~ 10^6 M^{-1}) which is located within the Forster radius distance of Trp-212 most likely corresponds to Site 2 (Fig. 1) in sub-domain IIIA. The next two binding sites with affinity values of ~ 10^5 M^{-1} are assigned to Site 1 in sub-domain IIA, which has a larger cavity than site 2 [20]. These FRET experiments on BSA, showed the presence of two extra binding sites which are difficult to detect by direct excitation (380 nm) of the complex because the ANS in these sites may have low fluorescence quantum yield. One of these BSA binding sites, where the binding constant is also ~ 10^5 M^{-1}, is located very close to Trp-134, in domain I. The lowest affinity binding site (~ 10^4 M^{-1}) is also the furthest away from both tryptophan residues which in this case can be assigned to sub-domain IIIB. The contribution from ANS molecules in this binding site is only likely to become significant at high BSA-ANS molar ratios. This is in contrast to the HSA-ANS complex where there are 3 sites [37].

If we assume that in the 1:1 BSA-ANS complex, the ANS is mainly bound to sites in sub-domain IIIA, then the distance between the closest tryptophan (Trp-212) and the ANS binding sites may increase during denaturation, and be observable via FRET. It is known that diazepam

DOI: 10.1007/s10895-009-0566-8

binds to domain III of HSA and a recent study showed that for HSA-diazepam complexes, GuHCl induced denaturation caused domain III to unfold first, without affecting the secondary structure of domain I and II [26]. A low stability energy of 1.4 kcal.mol^{-1} for HSA domain III was found by monitoring the fluorescence quenching of Trp by diazepam in HSA at different GuHCl concentrations. This energy is close to the value found in the first stage of three-state model (Table 1). In the 1:10 BSA-ANS complex, ANS molecules are also present in sub-domain IIA binding sites and this is observed as high FRET efficiency (quenching of Trp emission at 295 nm excitation, Fig. 4a, Increase in ANS emission, Fig. 4b) because Trp-212 is also located in the same sub-domain.

Using a combination of denaturation isotherm curves for the 1:10 BSA-ANS complex obtained by excitation at 295 nm (probing tryptophan fluorescence) and at 380 nm (probing the complex fluorescence) for the global analysis of the three-state model improves the accuracy of the unfolding parameters determined for sub-domain IIA. Therefore, we conclude that the second stage unfolding energy is most likely related to the stability of domain II in the BSA-ANS complex, as pointed out, with a stability energy similar to the unlabeled BSA, which was probed by observing the tryptophan fluorescence. It is important to note that a much higher energy for domain II stability or simply another cooperative transition could be found if one supposes that domain I in the serum albumin, which is the most stable one [26], is also being probed. Despite the possible presence of a bound ANS in domain I, which was assigned using FRET [10], it is likely that the low fluorescence intensity of this bound ANS is either due to more water molecule exposure or the decrease in binding affinity, which would make it difficult to be detected by steady-state methodology.

Time-resolved fluorescence.

A detailed fluorescence lifetime analysis of the BSA-ANS complexes was also undertaken and the kinetic parameters recovered from the use of a mixing of a single exponential and Gaussian lifetime distribution functions (eq. 11) are displayed in Tables 2 and 3 for the 1:1 and 1:10 complexes, respectively. In our previous work, where we analysed the decays using a double lifetime Gaussian distribution model we found that one of the distributions only changed very slightly during the denaturation process at both complex molar ratios [9]. This motivated us to simplify the analysis, and reanalyse the decay data using a combination of a single discrete lifetime plus a single Gaussian lifetime distribution. The justification is that the single exponential function probably accounts for the fluorescence of more external ANS which is more exposed to water, and thus has a short and narrow (~ 1-2 ns) lifetime distribution while the distribution term accounts for the ANS bound in a variety of micro-heterogeneous hydrophobic environments within the BSA (~ 2-17 ns). The chi squared values (Tables 2-3) and the residuals (not shown) for this new model have slightly improved by comparison to our previously reported study [9]. The key advantage, of this new lifetime analysis model is that all the heterogeneities where the ANS are bound to BSA can be described by a single Gaussian distribution function. For both complexes the main features of the lifetime analysis are that both decay time values, τ_1 and τ_2, decrease with increased denaturation, and the contribution of the short component increases while the long component decreases with increasing GuHCl concentration. This is explained in terms of increased exposure of bound ANS to water during the denaturation process [9]. The interesting aspect of the new analysis is the variation of the width of the Gaussian distribution and the maximum decay time for the Gaussian function with denaturant

DOI: 10.1007/s10895-009-0566-8

concentration (Figure 5-6).

The analysis of the time-resolved decay data in terms of a Gaussian lifetime distribution is a simpler model where the widths of the recovered lifetime distributions can be related to the degree of heterogeneity (and/or mobility) of the probe environment [9,38], and the mean values of the decay times to the degree of water exposure of the bound ANS. In the 1:1 complex (Fig. 5a), the distribution width increases up to a GuHCl concentration of ~1.5 M, but there are no significant changes in the lifetime value (τ_2 ~17 ns). This indicates an increase in the variety of micro-environments experienced by the bound ANS (due to a partial unfolding) but without a change in local polarity which indicates that the degree of unfolding is not large enough to change solvent access to the ANS. However, at 2.0 M we see a very significant change in the mean value of the distribution decay time (a decrease to ~ 13 ns), but without a change in the distribution width. At this denaturant concentration it is possible that a domain in the 1:1 BSA-ANS complex has now unfolded sufficiently to increase solvent exposure of the bound ANS but without changing the variety of different micro-environments at the binding site. This variety of micro-environments continues to be unchanged up to a GuHCl concentration of 2.5 M, after which the degree of unfolding becomes so significant that water molecule access to the bound ANS increases dramatically resulting in a decrease of τ_2 to around 8 ns. Further increases of denaturant concentration (> 2.5 M) make τ_2 oscillate between ~ 8 and 9 ns, while the distribution width decreases even further as the number of micro-environments decreases. If we assume that in the 1:1 BSA-ANS complex the ANS predominantly occupies binding site 2 (the hydrophobic cavity of sub-domain IIIA), this then strongly suggests that in the low denaturant concentration range (< 1.5M), it is domain III that undergoes structural changes, which either compresses the ANS binding site or causes the ANS fluorophores to move towards to the interior of the cavity. This compression causes an increased fluorescence emission intensity (due to increased separation from Trp-212), but the lifetime remains constant (no change in polarity), and the distribution remains relatively constant indicating no dramatic changes in the local environment. As the GuHCl concentration increases (> 2.0 M) the bound ANS becomes more exposed to the water molecules, but with increasing freedom.

The 1:10 BSA-ANS complex shows a similar overall behaviour, but with several significant differences (Fig 5b): i) The Gaussian distribution of the decay times are very different for 2.0 M and 2.5 M distributions, and ii) At high GuHCl concentrations (> 3.0 M) the lifetimes have shorter mean values. In the 1:10 complex, there are more ANS molecules which are dispersed amongst a variety of different binding sites, each of which has a different local polarity and is differentially sensitive to GuHCl denaturation. We can assume that at high molar ratio, binding site 1 is also occupied, one can suppose that the additional steep change of τ_2 from ~ 7 ns in 2.5 M GuHCl to ~ 2 ns for [GuHCl] > 3.0 M is a direct consequence of exposure of sub-domain IIA to the water solvent.

The difference between the two complexes is much more obvious when the maximum decay time for the Gaussian function versus denaturant concentration is plotted (Figure 6). It is interesting to note the similarity between these curves and the denaturation isotherm curves obtained from the steady-state experiments. In Fig. 6, both curves show a clear two stage denaturation process, however, in the 1:1 complex, the Gaussian function maximum value changes greatly from zero to 1.5 M while in the 1:10 complex the change is much less significant because of the additional bound ANS.

If we assume that the maximum value of the Gaussian distribution can be correlated to the

DOI: 10.1007/s10895-009-0566-8

occupancy of ANS in hydrophobic binding sites, then this can be directly correlated with protein concentration, we can then apply the three-state model globally (results are shown in table 4). The energy value of the first transition (~ 1 kcal.mol^{-1}) is in very good agreement with the value obtained from the steady-state data (Table 1). Note, however, that in the case of the second transition, the value of 7.8 kcal.mol^{-1} is significantly higher than that observed for steady state data. This indicates that some other interactions are also being detected in the lifetime data during this second transition, which are not observed in the steady state. It is most probable that this is due to the 1:10 BSA-ANS complex where ANS molecules are also located in domain I, and as such the stability energy determined from the lifetime data is related to the unfolding of both domain I and II. The stability energy of domain I, 7.4 kcal.mol^{-1}, has been previously determined using the fluorescence quenching of Hemin bound to domain I in HSA [11]. This value is very close to the energy of the second transition obtained by the time-resolved fluorescence analysis (table 4).

Conclusions

Our results show that bovine serum albumin denaturation by guanidinium hydrochloride (GuHCl) involves a two stage process with the formation of an intermediate state, which was observed and monitored by both steady-state and time-resolved fluorescence experiments. The fluorescence lifetime experiments proved to be more sensitive with regard to observing the presence of the intermediate states. The first, low energy unfolding step, involves the denaturation of domain III, or more precisely the area near binding site 2 (sub-domain IIIA) and the interface with sub-domain IIA. The second, high energy unfolding step involves domain II where the Trp-212 is located, *i.e.*, close to binding site 1 (sub-domain IIA). It is this second step which is likely to be the most observed and reported in the literature. The lifetime data clearly indicates differences in protein domain stability, and the probable presence of metastable intermediates, at different stages in the GuHCl induced denaturation of BSA. In a further development to our earlier work [9], we found that the combination of a discrete and a Gaussian lifetime term in the analysis model proved to be a simpler method for elucidating the sequence of unfolding events, and generating accurate thermodynamic data. We hope to apply this lifetime analysis model to facilitate the detection of possible intermediates in the denaturation of homologous proteins such as Human Serum Albumin where there has been some debate in the literature regarding the presence of intermediate(s) during chemical denaturation.

Acknowledgments:
This work was supported by funding from Science Foundation Ireland (Principal Investigator grant number 02/IN.1/M231 to AGR) and the National Biophotonics Imaging Platform, an Irish Higher Education Authority Programme for Research in Third Level Institutions supported project.

DOI: 10.1007/s10895-009-0566-8

Table 1 – Thermodynamic parameters for BSA and BSA-ANS denaturation by GuHCl generated from steady-state fluorescence data fitted to two and three-state models.

Parameters	BSA (1:0)[a)]	BSA-ANS (1:1)[a)]	BSA-ANS (1:10)[a)]	BSA-ANS (1:1)[b)]	BSA-ANS (1:10)[b)]
$-m_I$ / kcal.mol^{-1}.M^{-1}	—	1.7 ± 0.4[c]	1.7 ± 0.4[c]	1.7 ± 0.4[c]	1.7 ± 0.4[c]
$-m_D$ / kcal.mol^{-1}.M^{-1}	2.5 ± 0.2	5.3 ± 0.5[c]	5.3 ± 0.5[c]	5.3 ± 0.5[c]	5.3 ± 0.5[c]
$\Delta G^0_{H_2O,I}$ / kcal.mol^{-1}	—	0.9 ± 0.2[c]	0.9 ± 0.2[c]	0.9 ± 0.2[c]	0.9 ± 0.2[c]
$\Delta G^0_{H_2O,D}$ / kcal.mol^{-1}	4.5 ± 0.4	6.7 ± 0.4[c]	6.7 ± 0.4[c]	6.7 ± 0.4[c]	6.7 ± 0.4[c]
α_N / M^{-1}	0.02 ± 0.02	0.2 ± 0.1	-0.1 ± 0.2	-0.7 ± 0.2	-0.3 ± 0.2
α_I / M^{-1}	—	0[d]	0[d]	0[d]	0[d]
α_D / M^{-1}	-0.01 ± 0.01	0[d]	0[d]	0[d]	0[d]
I^0_N / a.u.	1.01 ± 0.01	0.72± 0.03	0.01 ± 0.03	1.16 ± 0.05	1.11 ± 0.04
I^0_I / a.u.	—	0.91 ± 0.04	0.39 ± 0.04	0.37 ± 0.05	0.52 ± 0.04
I^0_D / a.u.	0.39 ± 0.03	0.35 ± 0.01	0.28 ± 0.01	0.03 ± 0.01	0.02 ± 0.01

a) Excitation at 295 nm. b) Excitation at 380 nm. c) Globally adjusted, and d) fixed values. Two-state model, r^2 = 0.9994, and three state model, r^2 =0.9978.

DOI: 10.1007/s10895-009-0566-8

Table 2 – Decay parameters of lifetime Gaussian distribution and exponential fit of (1:1) BSA-ANS complex fluorescence at different GuHCl concentration using 405nm excitation and 480 nm emission.

[GuHCl] / M	$\tau_{\square}$ / ns	τ_2 / ns	σ_1 / ns	a_1	a_2	χ^2 §
0	16.89	2.14	5.93	0.0975	0.0223	1.100
0.5	17.07	2.28	6.16	0.0735	0.0241	1.116
1.0	16.92	2.24	6.63	0.0567	0.0245	1.144
1.5	16.63	2.04	7.08	0.0394	0.0263	1.091
2.0	13.36	1.97	6.99	0.0129	0.0286	1.231
2.5	7.70	1.70	6.94	0.0057	0.0250	1.195
3.0	8.71	1.75	4.20	0.0033	0.0296	1.169
3.5	7.79	1.61	3.26	0.0022	0.0284	1.224
4.0	8.32	1.69	2.08	0.0020	0.0309	1.270
4.5	7.93	1.66	2.99	0.0026	0.0318	1.180
5.0	8.27	1.68	2.58	0.0021	0.0319	1.255

§ The average value is 1.180

Table 3 – Decay parameters of lifetime Gaussian distribution and exponential fit of the (1:10)- BSA-ANS complex fluorescence at different GuHCl concentration using 405nm excitation and 480 nm probe emission.

[GuHCl] / M	$\tau_{\square}$ / ns	τ_2 / ns	σ_1 / ns	a_1	a_2	χ^2 §
0	16.45	1.82	6.84	0.1280	0.0168	1.166
0.5	16.44	1.82	6.81	0.1240	0.0116	1.069
1.0	16.75	1.38	7.02	0.1222	0.0142	1.098
1.5	16.63	1.41	7.14	0.1064	0.0184	1.109
2.0	11.12	0.88	8.24	0.0246	0.0276	1.124
2.5	7.20	0.87	8.56	0.0128	0.0270	1.059
3.0	2.01	0.82	11.15	0.0119	0.0274	1.090
3.5	2.01	0.86	9.26	0.0076	0.0331	1.091
4.0	1.89	0.88	8.71	0.0064	0.0382	1.090
4.5	1.69	0.79	7.69	0.0061	0.0438	1.195
5.0	1.74	0.95	7.98	0.0052	0.0377	1.149

§ The average value is 1.106

DOI: 10.1007/s10895-009-0566-8

Table 4 – Thermodynamic parameters for BSA-ANS denaturation by GuHCl generated from a global fit of a stage model analysis of decay times Gaussian distribution.

BSA-ANS	$-m_I$ / kcal.mol^{-1}.M^{-1}	$-m_D$ / kcal.mol^{-1}.M^{-1}	$\Delta G^0_{H_2O,I}$ / kcal.mol^{-1}	$\Delta G^0_{H_2O,D}$ / kcal.mol^{-1}
(1:1)[a] and (1:10)[b]	1.2 ± 1.3	5.1 ± 1.3	1.0 ± 3.8	7.8 ± 2.7

(a) α_N = (-0.004 ± 0.01) M^{-1}; $\alpha_I = \alpha_D$ = 0 M^{-1} (fixed); I^0_N = (0.010± 0.008); I^0_I = (0.004 ± 0.006); I^0_D = (0.004 ± 0.006); (b) α_N = (-0.001 ± 0.002) M^{-1}; $\alpha_I = \alpha_D$ = 0 M^{-1} (fixed); I^0_N = (0.011 ± 0.001); I^0_I = (0.010± 0.002); I^0_D = (0.0005 ± 0.0001); (c) Globally adjusted. r^2 =0.9994.

Figures

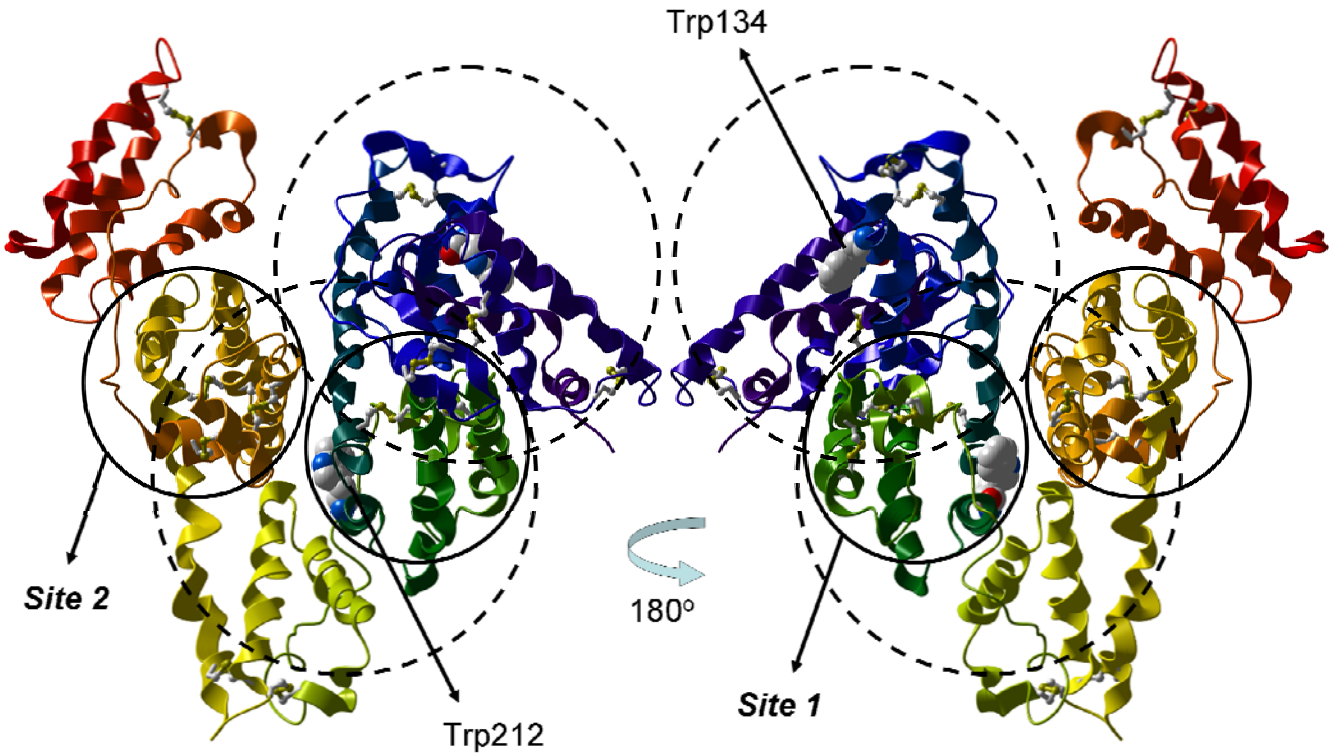

Figure 1 – Two side-on 3D graphic representation of a BSA model structure based on HSA x-ray crystal structure obtained from the Protein Data Bank (PDB ID: 1UOR) [18]. The unbroken circles show the binding sites described by Ghuman *et al*. [20] which are located in sub-domains IIA and IIIA, respectively. The dashed circles centred at the tryptophan residues show the distance limit for 50% FRET efficiency [10].

DOI: 10.1007/s10895-009-0566-8

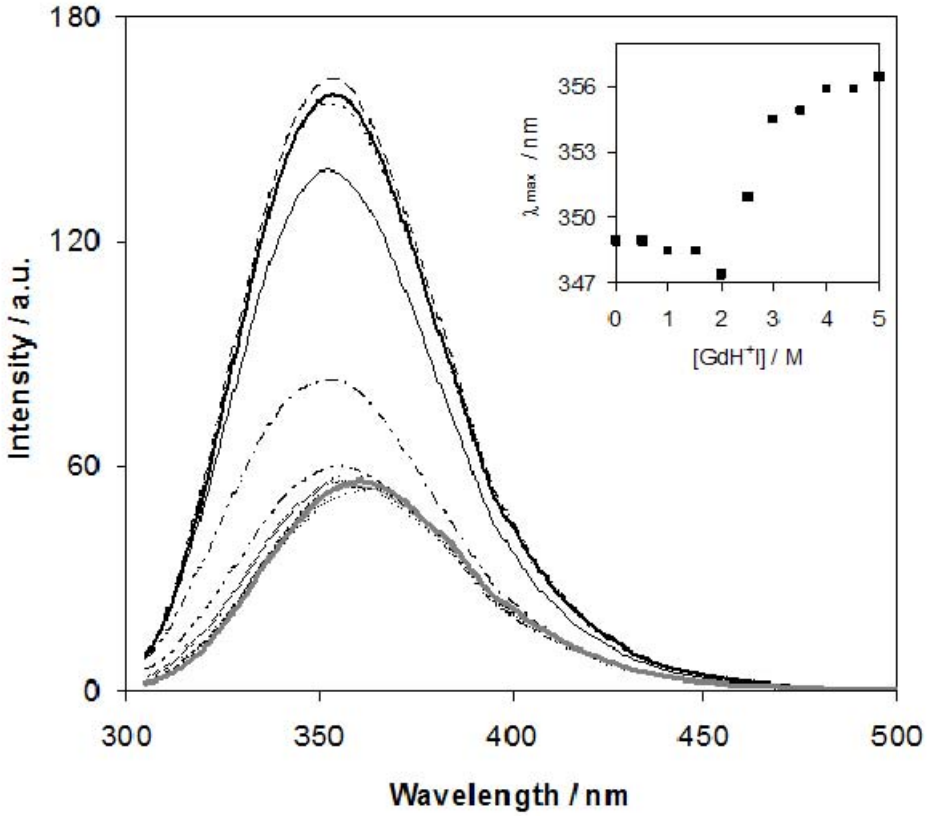

Figure 2 – A series of fluorescence spectra showing the denaturation of unlabeled BSA by Guanidinium Hydrochloride (GuHCl) in PBS buffer at pH=7.4 and 25°C. The excitation wavelength was 295 nm. Inset shows the change in the position of fluorescence intensity maximum with respect to increasing GuHCl concentration.

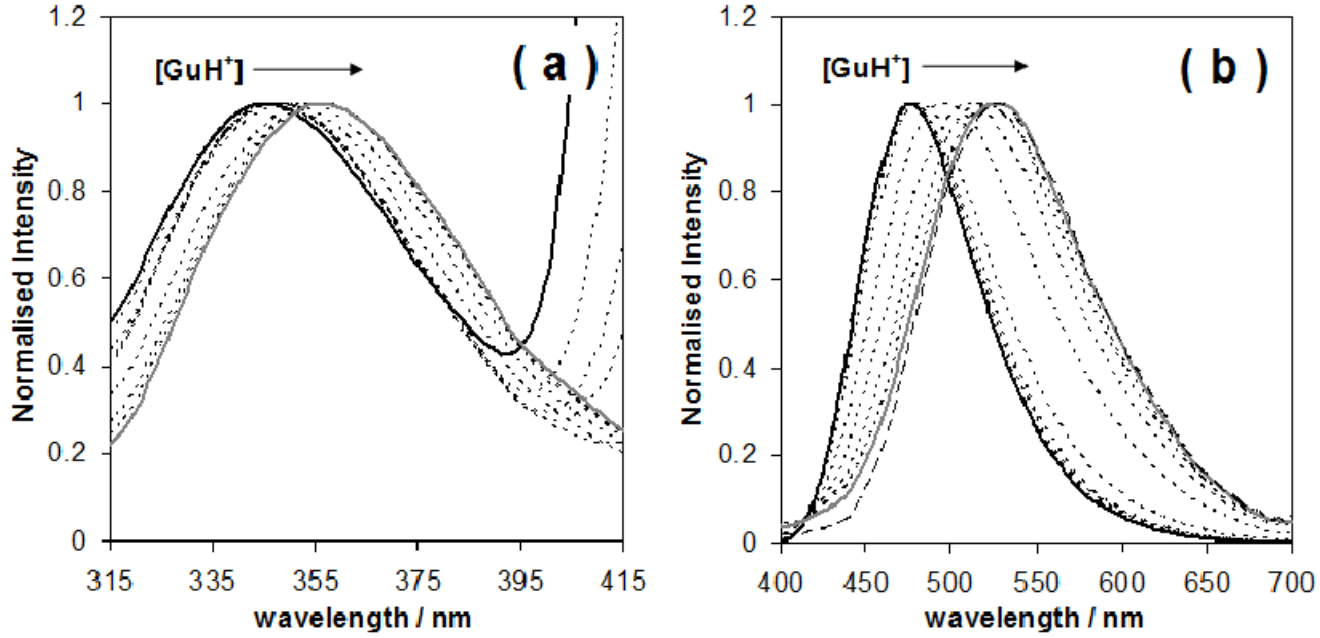

Figure 3 – Normalised fluorescence emission spectra of the (1:10) BSA-ANS complex in PBS at pH=7.4, using (a) 295 nm excitation, Trp emission and (b) 380 nm excitation, ANS emission. The *heavy black lines* are BSA-ANS emission with [GuHCl] = 0 M. The *dotted line* spectra represent BSA-ANS with increasing GuHCl concentration, while the heavy grey line represents

DOI: 10.1007/s10895-009-0566-8

the 5M case. The fluorescence spectrum of $4x10^{-6}$ M ANS in 5 M GuHCl is shown as a *dashed line* curve in (b).

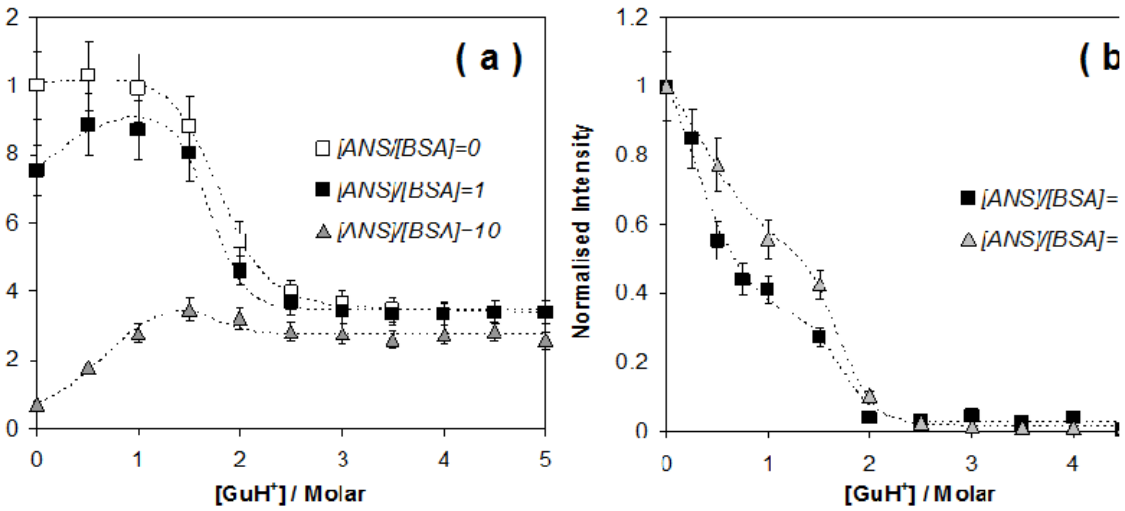

Figure 4 – Effect of GuHCl in PBS solution at pH=7.4: on (a) the Trp fluorescence emission excited at 295 nm and detected at 350 nm for BSA, 1:1 BSA-ANS, and 1:10 BSA-ANS complexes. The Trp fluorescence emission from the complexes were normalised relative to the Trp emission of the unlabeled BSA at zero GuHCl concentration; and on (b) the ANS emission, excited at 380 nm in the 1:1 and 1:10 BSA-ANS complexes. The dotted lines represent the best model curve fits (see text).

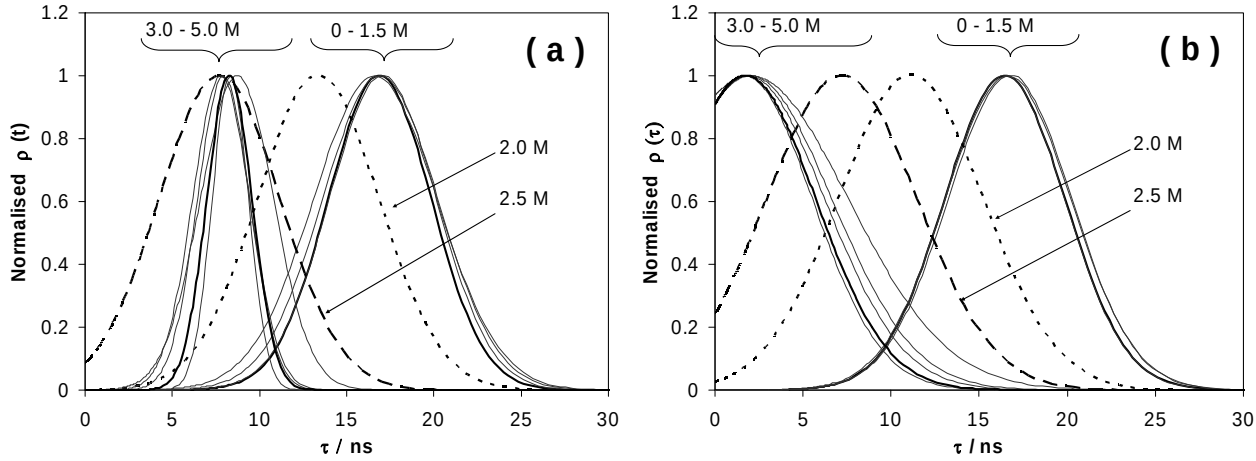

Figure 5 – The Gaussian distribution of decay times associated to the long fluorescence lifetime of (a) the 1:1 BSA-ANS, and (b) the 1:10 BSA-ANS complexes. The solid black line curves with the highest and lowest τ values are BSA-ANS with 0 M, and 5.0 M GuHCl, respectively. The dotted line curves represent BSA-ANS with 2.0 M GuHCl, while the dashed line curves are the complexes with 2.5 M GuHCl. The distributions measured for increasing concentrations of GuHCl in each of those regions (0 M to ~2 M, and 2/2.5 M to 5 M) are represented by grey line spectra (see text).

DOI: 10.1007/s10895-009-0566-8

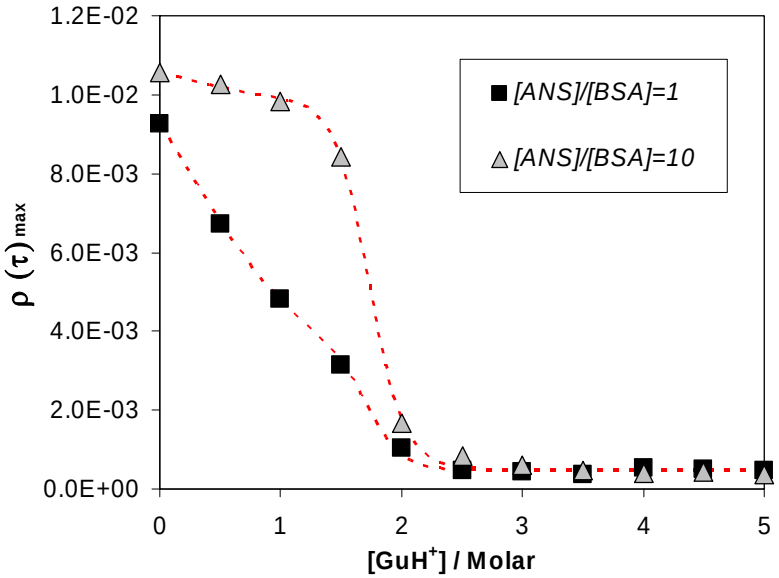

Figure 6 – Effect of GuHCl in PBS solution at pH=7.4 on the maximum decay time of the Gaussian distribution of the long lifetime component, obtained from the time-resolved fluorescence decays of the 1:1 BSA-ANS and 1:10 BSA-ANS complexes. The dotted lines represent the three-state model curve global fitting.

References

[1] V. Daggett and A. Fersht, (2003), The present view of the mechanism of protein folding, Nat. Rev. Mol. Cell. Biol. 4, 497-502

[2] G. Taubes, (1996), Misfolding the way to disease, Science 271, 1493-1495

[3] C. M. Dobson, (2004), Principles of protein folding, misfolding and aggregation, Siminars in Cell & Developmental Biology 15, 3.

[4] T. O. Street, N. Courtemanche, and D. Barrick (2008), Protein Folding and Stability Using Denaturants, Methods in Cell Biology, Editors: J.J. Correia and H.W. Detrich, III, Academic Press, London, vol. 84 ch 11, pgs 295-325.

[5] K.A. Dill and D. Shortle, (1991), Denatured states of proteins, Annu. Rev. Biochem. 60, 795-825

[6] J.-H. Han, S. Batey, A. A. Nickson, S.A. Teichmann, and J. Clarke (2007) The folding and evolution of multidomain proteins, Nature Reviews Molecular Cell Biology 8, 319-330

[7] S. Batey, K. A. Scott, and J. Clarke (2006) Complex Folding Kinetics of a Multidomain Protein, Biophys. J. 90, 2120-2130.

[8] Lakowicz, J.R. "Principles of Fluorescence Spectroscopy." 2006. Springer 3rd ed, Singapore. Ch. 3 and 16.

[9] D.M Togashi and A.G. Ryder (2006) Time-Resolved Fluorescence Studies on Bovine Serum Albumin Denaturation Process, J. Fluoresc. 16, 153-160.

[10] D.M Togashi and A.G. Ryder (2008) A Fluorescence Analysis of ANS Bound to Bovine Serum Albumin: Binding Properties Revisited by Using Energy Transfer, J. Fluoresc. (2008) 18:519–526.

[11] A. K. Shaw and S. K. Pal (2008) Resonance energy transfer and ligand binding studies on pH induced folded states of human serum albumin, J. Photochem. Photobio. B 90, 187-197

[12] O. K. Abou-Zied and O. I.K. Al-Shihi (2008) Characterization of Subdomain IIA Binding Site of Human Serum Albumin in its Native, Unfolded, and Refolded States using small molecular probes, J. Am. Chem. Soc. 130, 10793-10801

[13] S.S. Krishnakumar and D. Panda (2002) Spatial Relationship between the Prodan Site, Trp-214, and Cys-34 residues in Human Serum Albumin and Loss of Structure through incremental Unfolding, Biochemistry, 41, 7443-7452.

DOI: 10.1007/s10895-009-0566-8

[14] M. Cardamone and N.K. Puri, (1992), Spectrofluorimetric assessment of the surface hydrophobicity of proteins, Biochem. J. 282, 589-593
[15] L. Brand and J.R. Gohlke, (1972) Fluorescence probes for structure, Annu. Rev. Biochem. 41, 843-868
[16] G. Weber and L.B. Young, (1964) Fragmentation of bovine serum albumin by pepsin .1. Origin of acid expansion of albumin molecule, J. Biol. Chem. 239 1415-1423
[17] D.M. Togashi and A.G. Ryder, (2007) Fluorescence lifetime imaging study of a thin protein layer on solid surfaces, Exp. Mol. Pathol. 82 (2), 135-41
[18] X.M. He and D.C. Carter (1992) Atomic-structure and chemistry of human serum-albumin, Nature 358, 209-215
[19] T. Perters and Jr (1996) All about Albumin. Academic Press, USA.
[20] J. Ghuman, P.A. Zunszain, I. Petitpas, A.A. Bhattacharya, M. Otagiri, and S. Curry (2005) J. Mol. Biol. 353, 38-52.
[21] B. Farruggia and G.A. Picó (1999) Thermodynamic features of the chemical and thermal denaturations of human serum albumin, Int. J. Biol. Macromol. 26(5) 317-323
[22] S. Muzammil, Y. Kumar, and S. Tayyab (2000) Anion-induced stabilization of Human Serum Albumin Prevents the Formation of Intermediate During Urea Denaturation, Proteins: Struct. Funct. Genet. 40, 29-38
[23] S. Tayyab, M.U. Siddiqui, and N. Ahmad (1995) Experimental Determination of the Free Energy of Unfolding of Proteins, Biochem. Ed. 23, 162-164
[24] B. Farruggia, F. Rodriguez, R. Rigatuso, G. Fidelio, and G. Pico (2001) The participation of Human Serum Albumin Domains in Chemical and Thermal Unfolding, J. Protein Chem. 20(1) 81-89.
[25] K. Flora, J.D. Brennan, G.A. Baker, M.A. Doody, and F.V. Bright (1998), Unfolding of Acrylodan-Labeled Human Serum Albumin Probed by Steady-state and Time-resolved Fluorescence Methods, Biophys. J. 75, 1084-1096
[26] B. Ahmad, M. Z. Ahmed, S. K. Haq, and R. H. Khan (2005) Guanidine Hydrochloride denaturation of human serum albumin originates by local unfolding of some stable loops in domain III, Biochim. Biophys. Acta Proteins and proteomics. 1750 (1) 93-102.
[27] M.K. Santra, A. Banerjee, O. Rahaman, and D. Panda (2005) Unfolding pathways of human serum albumin: Evidence for sequential unfolding and folding of its three domains Int. J. Biol. Macromol 37, 200-204.
[28] M.,K. Santra, A. Banerjee, S.S. Krishnakumar, O. Rahaman, and D. Panda (2004) Multile-Probe analyis of folding and unfolding pathways of human serum albumin. Evidence for a framework mechanism of folding, Eur. J. Biochem. 271, 1789-1797
[29] L.-Z. Wu, B.-L. Ma, D.-W. Zou, Z.-X. Tie, J. Wang, and W. Wang, (2008) Influence of metal ions on folding pathway and conformational stability of bovine serum albumin J. Mol. Struct. 877, 44-49
[30] M.M. Santoro and D.W. Bolen (1988) Unfolding Free Energy Changes Determinde by the Linear Extrapolation Method. 1. Unfolding of Phenylmethanosulfonyl a-Chymotrypsin Using Different Denaturants, Biochemistry 27, 8063-8068
[31] B. John, P. R. D'Silva, and A.K. Lala (2001) Analysis of protein folding using polarity-sensitive fluorescent probes Curr. Sci. 80(2) 287-290
[32] A. Sulkowska, J.Rownicka, B.Bojko, J.Pozycka, I.Zubik-Skupien, and W. Sulkowski (2004) Effect of guanidine hydrochloride on bovine serum albumin complex with antithyroid drugs: fluorescence study. J. Mol. Struct. 704, 291-295
[33] Y. Chen and M.D. Barkley (1998) Toward understanding tryptophan fluorescence in proteins. Biochemistry 37(28) 9976-9982.
[34] W. Qiu, T. Li, L. Zhang, Y. Yang, Y.-T. Kao, L. Wang, and D. Zhong (2008) Ultrafast quenching of tryptophan fluorescence in proteins: Interresidue and intrahelical electron transfer, Chem. Phys. 350, 154-164
[35] S.M. Andrade and S.M.B. Costa (2000) The Location of Tryptophan, N-acetyltryptophan and α-Chymotrypsin in Reverse Micelles of AOT: A Fluorescence Study, Photochem. Photobiol. 72(4):444-450.

DOI: 10.1007/s10895-009-0566-8

[36] In the tryptophan excitation, the fluorescence emission of all the intensities are normalised to the fluorescence intensity of unlabeled BSA.
[37] L.A. Bagatolli, S.C. Kivatinitz, F. Aguilar, M.A. Soto, P. Sotomayor, and G.D. Fidelio (1996) Two Distinguishable Fluorescent Modes of 1-Anilino-8-Naphtalenesulfonate Bound to Human Albumin, J. Fluoresc. 6, 33-40
[38] M.K. Helms, C.E. Petersen, N.V. Bhagavan, and D.M. Jameson, (1997), Time-resolved fluorescence studies on site-directed mutants of human serum albumin, *FEBES Lett.* 408, 67-70

DOI: 10.1007/s10895-009-0566-8